Pergamon

Renewable Energy, Vol. 6, No. 7, pp. 725–738, 1995

0960-1481/95 $9.50+0.00

0960–1481(94)00099–9

NOVEL TWO-DIMENSIONAL TRANSMISSION-LINE COLLECTION SYSTEMS FOR PHOTOVOLTAIC POWER

MING YING KUO, CHING CHUAN KUO AND MEI SHONG KUO
Institute of Electronics, National Chiao Tung University, Taiwan, People's Republic of China

(*Received* 18 *November* 1994; *accepted* 18 *December* 1994)

Abstract—Innovative two-dimensional transmission-line systems for collecting distributed photovoltaic power are presented in this paper. Based on transmission-line theory and controlling the phase of a.c. sources, the net power of the proposed transmission-line type network can flow towards the target load. The validity of the proposed system is confirmed by mathematical analysis and simulated results. This paper makes a contribution to the concept of networks for the collection of renewable energy.

1. INTRODUCTION

The generation of electrical energy faces many problems today. In a world of growing environmental awareness, nuclear power plants find less and less acceptance and conventional power plants are criticized due to their CO_2 emissions. The natural world is filled with a large amount of clean and safe renewable energy, and regenerative energy systems are therefore becoming more important then ever. One natural way of converting sunlight into d.c. electricity is by photovoltaic (PV) cells. PV power has more and more potential to compete with conventional central power plants as decades of research have lowered the cost and boosted the efficiency of PV cells [1].

High power PV systems, which can be constructed by directly connecting PV modules in series and/or in parallel, have some problems due to the effect of variations in irradiance, manufacturing and temperature on the I–V characteristics of a PV cell. The first problem, protection against less efficient modules absorbing the power of all other modules, can be solved by adding blocking and/or bypass diodes. However, these diodes introduce energy losses, which can be non-negligible in the case of a large network [2]. The second is that it is impossible for every module to operate on its maximum power point for series and/or parallel arrangements of modules. In other words, the maximum power received by the load will be less than the sum of the maximun powers supplied by individual modules. Therefore, the lower efficiency must also be considered for these kinds of PV power systems.

Another kind of high power PV system could be created by directly connecting d.c. to d.c.-current-source converters in parallel or directly connecting d.c. to d.c.-voltage-source converters in series. The power from the PV module/array is converted into a d.c. current source or a d.c. voltage source by a highly efficient d.c. to d.c. converter with maximum power point tracking (MPPT) [3]. The MPPT function of a d.c. to d.c. converter guarantees that every module operates on its maximun power point and the efficiency of the whole system is further improved. However, the electric stress applied to every d.c. to d.c. converter will increase as the number of converters is increased, which implies higher costs to be considered.

Innovative transmission-line collection networks for PV power with lower cost and high efficiency are proposed in this paper. Photovoltaic power can be converted into a.c. electricity by a d.c. to a.c. converter with MPPT. These collection systems are constructed from a large number of d.c. to a.c. converters which are dispersed over a very large area and are connected by a transmission line network. The power from the renewable PV sources is naturally transmitted into the target load via the transmission-line collection network by using the theory of transmission lines and the phase relation between the sinusoidal outputs of the converters [4]. Based on mathematical analysis, the electric stress of only those d.c. to a.c. converters which are closer to the target load is larger, therefore, the total cost of the proposed power collection systems can be reduced effectively.

In order to simplify the complicated mathematical analysis, it is assumed that all d.c. to a.c. converters with MPPT are ideal a.c. electric sources throughout this paper. Section 2 presents the current-type transmission-line collection system (CT-TLCS) and the

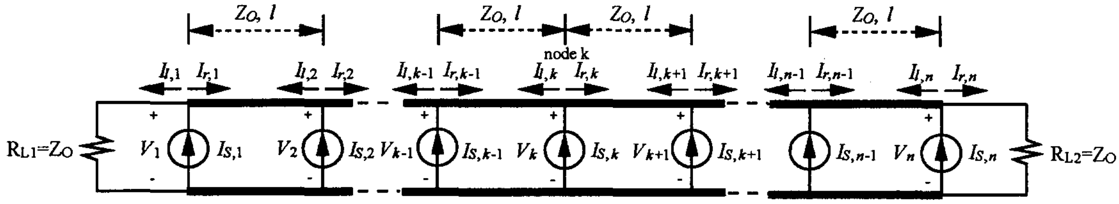

Fig. 1. Current-type transmission line collection system (CT-TLCS).

emphasis is that the electrical properties of the proposed collection system are analyzed under both important accumulation conditions. Section 3 addresses the transmission-line type voltage source (TLT-VS) constructed from a.c. current sources and transmission lines. Section 4 shows the development of a voltage-type transmission-line collection system (VT-TLCS) and a transmission-line type current source (TLT-CS), based on the principle of network duality. Section 5 proposes innovative two-dimensional transmission-line collection systems (2D-TLCSs), the importance of which is that the simulated results can be used to facilitate the realization of 2D-TLCSs.

2. CURRENT-TYPE TRANSMISSION LINE COLLECTION SYSTEM

The collection system with distributed current sources is called a current-type transmission-line collection system (CT-TLCS) and is shown in Fig. 1, where Z_0 and l denote, respectively, the characteristic impedance and the length of the subtransmission line and there are matching conditions at both load terminals, that is, $R_{L1} = R_{L2} = Z_0$. The internal impedance of the current source used in this paper is assumed to be much larger than Z_0 and is therefore negligible. The phasor representation of a current source, $i_{S,k}(t) = I_m \cos(2\pi ft+k\theta)$, is defined as $I_{S,k} = I_m \times e^{jk\theta}$, where I_m and f are, respectively, the amplitude and the frequency of source.

The CT-TLCS in Fig. 1 can be regarded as a linear system since lossless transmission lines are linear; therefore, the principle of superposition holds. First, Fig. 2 illustrates that the output responses, I_k and V_k, to the mth current source, $I_{S,m}$, are considered while the other sources are set to zero. Based on the lossless transmission line (TL) theory, I_k and V_k are expressed as [4],

$$V_k = Z_0[i_0^+ e^{-j\beta(k-m)l} + i_0^- e^{j\beta(k-m)l}], \tag{1}$$

and

$$I_k = i_0^+ e^{-j\beta(k-m)l} - i_0^- e^{j\beta(k-m)l}, \tag{2}$$

where i_0^+ and i_0^- are, respectively, the incident wave and reflected wave, and the phase constant β is given by

$$\beta = \frac{2\pi}{\lambda} = \frac{2\pi f}{u_p}, \tag{3}$$

where λ and u_p are the wavelength and phase velocity of the lossless TL with respect to f. Since the matching conditions hold at R_{L1} and R_{L2}, the input impedances $Z_{l,m}$ and $Z_{r,m}$ are equal to Z_0 and, simultaneously, the reflective wave i_0^- equals zero. Consequently, the equation $i_0^+ = \frac{1}{2}I_{S,m}$ is obtained by applying Kirchhoff's current law to node m. Therefore, I_k and V_k are obtained as follows

$$V_k = \tfrac{1}{2}Z_0 I_{S,m} e^{-j\beta(k-m)l}, \tag{4}$$

and

$$I_k = \tfrac{1}{2}I_{S,m} e^{-j\beta(k-m)l}. \tag{5}$$

Now, as the principle of superposition is valid for the CT-TLCS in Fig. 1, the total effect on any output due to all the current sources acting simultaneously

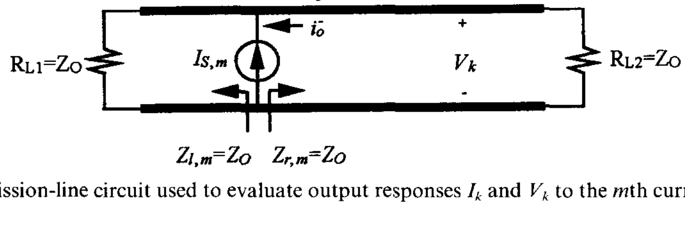

Fig. 2. Transmission-line circuit used to evaluate output responses I_k and V_k to the mth current source $I_{S,m}$.

can be obtained by adding the individual effects. Based on eqs (4) and (5), the outputs $I_{r,k}$, $I_{l,k}$, and V_k are therefore related with all the sources by

$$I_{r,k} = \tfrac{1}{2}I_{S,1}\,e^{-j\beta(k-1)l} + \cdots + \tfrac{1}{2}I_{S,k-1}\,e^{-j\beta l} + \tfrac{1}{2}I_{S,k} - \tfrac{1}{2}I_{S,k+1}\,e^{-j\beta l} - \cdots - \tfrac{1}{2}I_{S,n}\,e^{-j\beta(n-k)l}, \quad (6)$$

$$I_{l,k} = -\tfrac{1}{2}I_{S,1}\,e^{-j\beta(k-1)l} - \cdots - \tfrac{1}{2}I_{S,k-1}\,e^{-j\beta l} + \tfrac{1}{2}I_{S,k} + \tfrac{1}{2}I_{S,k+1}\,e^{-j\beta l} + \cdots + \tfrac{1}{2}I_{S,n}\,e^{-j\beta(n-k)l}, \quad (7)$$

and

$$V_k = \tfrac{1}{2}Z_0[I_{S,1}\,e^{-j\beta(k-1)l} + \cdots + I_{S,k-1}\,e^{-j\beta l} + I_{S,k} + I_{S,k+1}\,e^{-j\beta l} + \cdots + I_{S,n}\,e^{-j\beta(n-k)l}], \quad (8)$$

where the negative sign in eqs (6) and (7) indicates the direction of $I_{r,k}$ or $I_{l,k}$ to be opposite to the output response of the source. The CT-TLCS is required to propagate energy to one terminal and propagate no energy to the other terminal. In other words, either V_1 or V_n will be zero. Substituting $I_{S,k} = I_m e^{jk\theta}$ into eq. (8) and letting $\beta l = \theta$, V_1 and V_n are written as

$$V_1 = \frac{n}{2}Z_0 I_m\,e^{j\theta}, \quad (9)$$

and

$$V_n = \tfrac{1}{2}Z_0 I_m(e^{-j(n-2)\theta} + e^{-j(n-4)\theta} + e^{-j(n-6)\theta} + \cdots + e^{jn\theta}). \quad (10)$$

It is noted that when $\beta l = \theta = \pi/n$, V_n is equal to zero, but V_1 is not, which implies that the CT-TLCS transmits power to R_{L1} but transmits no power to R_{L2}. Similarly, by letting $\beta l = -\theta$, V_1 and V_n are expressed as

$$V_1 = \tfrac{1}{2}Z_0 I_m(e^{j\theta} + e^{j3\theta} + e^{j5\theta} + \cdots + e^{jn\theta}), \quad (11)$$

and

$$V_n = \frac{n}{2}Z_0 I_m\,e^{jn\theta}. \quad (12)$$

The importance is that when $\beta l = -\theta = \pi/n$, V_1 equals zero but V_n does not, which implies that the CT-TLCS transmits power to R_{L2} but transmits no power to R_{L1}. In addition, the length, l, of every subTL notably equals $\lambda/2n$, as obtained by combining $\beta l = \pi/n$ with eq. (3).

Since $\beta l = \pi/n$, all the outputs of $I_{r,k}$, $I_{l,k}$ and V_k can be expressed as the form of matrices:

$$\begin{bmatrix} I_{r,1} \\ I_{r,2} \\ I_{r,3} \\ \vdots \\ I_{r,n} \end{bmatrix} = \begin{bmatrix} 1 & -e^{-j\frac{\pi}{n}} & -e^{-j\frac{2\pi}{n}} & \cdots & -e^{-j\frac{(n-1)\pi}{n}} \\ e^{-j\frac{\pi}{n}} & 1 & -e^{-j\frac{\pi}{n}} & \cdots & -e^{-j\frac{(n-2)\pi}{n}} \\ e^{-j\frac{2\pi}{n}} & e^{-j\frac{\pi}{n}} & 1 & \cdots & -e^{-j\frac{(n-3)\pi}{n}} \\ \vdots & \vdots & \vdots & \ddots & \vdots \\ e^{-j\frac{(n-1)\pi}{n}} & e^{-j\frac{(n-2)\pi}{n}} & e^{-j\frac{(n-3)\pi}{n}} & \cdots & 1 \end{bmatrix} \begin{bmatrix} \frac{1}{2}I_{S,1} \\ \frac{1}{2}I_{S,2} \\ \frac{1}{2}I_{S,3} \\ \vdots \\ \frac{1}{2}I_{S,n} \end{bmatrix}, \quad (13)$$

$$\begin{bmatrix} I_{l,1} \\ I_{l,2} \\ I_{l,3} \\ \vdots \\ I_{l,n} \end{bmatrix} = \begin{bmatrix} 1 & e^{-j\frac{\pi}{n}} & e^{-j\frac{2\pi}{n}} & \cdots & e^{-j\frac{(n-1)\pi}{n}} \\ -e^{-j\frac{\pi}{n}} & 1 & e^{-j\frac{\pi}{n}} & \cdots & e^{-j\frac{(n-2)\pi}{n}} \\ -e^{-j\frac{2\pi}{n}} & -e^{-j\frac{\pi}{n}} & 1 & \cdots & e^{-j\frac{(n-3)\pi}{n}} \\ \vdots & \vdots & \vdots & \ddots & \vdots \\ -e^{-j\frac{(n-1)\pi}{n}} & -e^{-j\frac{(n-2)\pi}{n}} & -e^{-j\frac{(n-3)\pi}{n}} & \cdots & 1 \end{bmatrix} \begin{bmatrix} \frac{1}{2}I_{S,1} \\ \frac{1}{2}I_{S,2} \\ \frac{1}{2}I_{S,3} \\ \vdots \\ \frac{1}{2}I_{S,n} \end{bmatrix}, \quad (14)$$

and

$$\begin{bmatrix} V_1 \\ V_2 \\ V_3 \\ \vdots \\ V_n \end{bmatrix} = Z_0 \times \begin{bmatrix} 1 & e^{-j\frac{\pi}{n}} & e^{-j\frac{2\pi}{n}} & \cdots & e^{-j\frac{(n-1)\pi}{n}} \\ e^{-j\frac{\pi}{n}} & 1 & e^{-j\frac{\pi}{n}} & \cdots & e^{-j\frac{(n-2)\pi}{n}} \\ e^{-j\frac{2\pi}{n}} & e^{-j\frac{\pi}{n}} & 1 & \cdots & e^{-j\frac{(n-3)\pi}{n}} \\ \vdots & \vdots & \vdots & \ddots & \vdots \\ e^{-j\frac{(n-1)\pi}{n}} & e^{-j\frac{(n-2)\pi}{n}} & e^{-j\frac{(n-3)\pi}{n}} & \vdots & 1 \end{bmatrix} \begin{bmatrix} \frac{1}{2}I_{S,1} \\ \frac{1}{2}I_{S,2} \\ \frac{1}{2}I_{S,3} \\ \vdots \\ \frac{1}{2}I_{S,n} \end{bmatrix}. \quad (15)$$

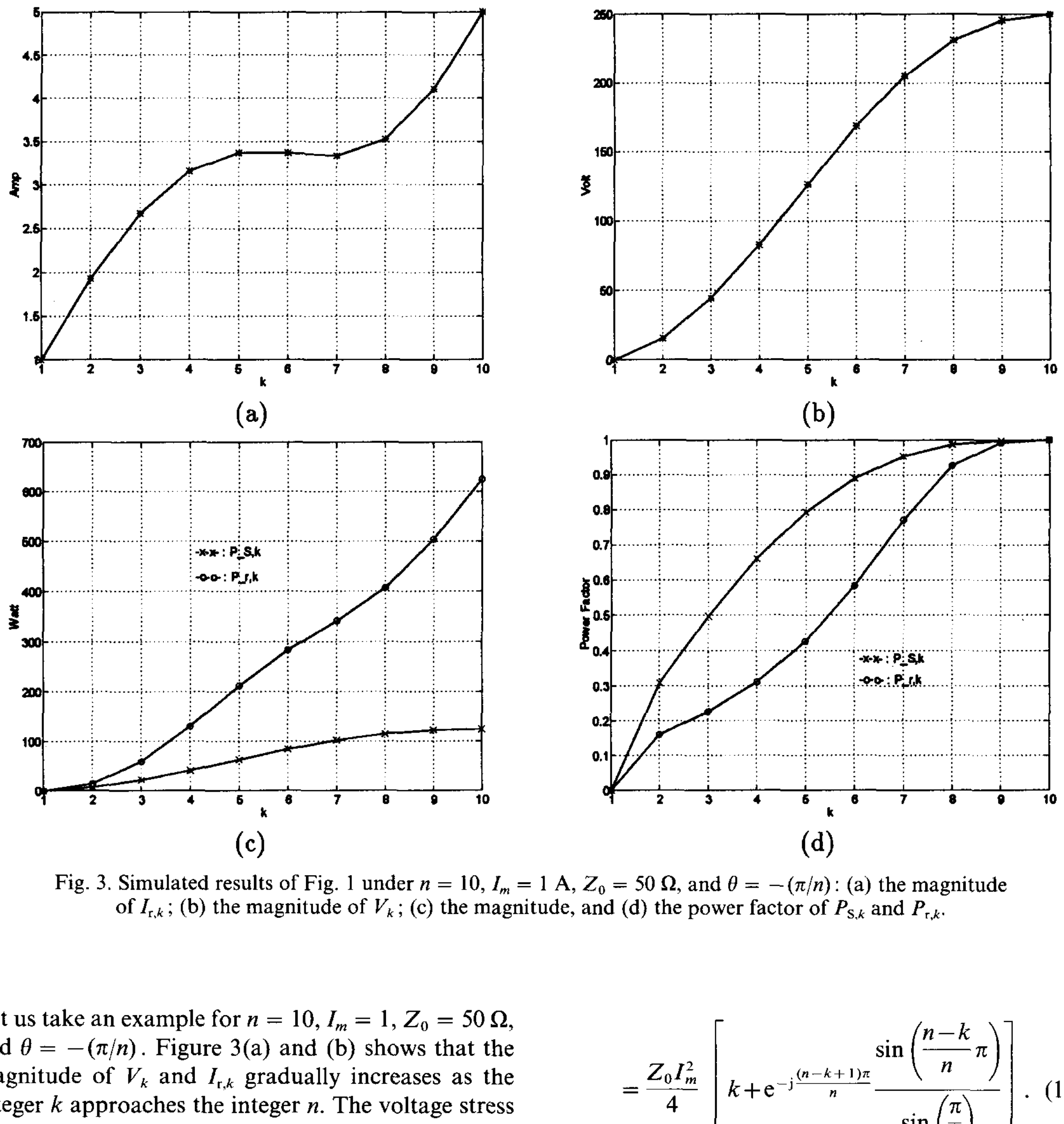

Fig. 3. Simulated results of Fig. 1 under $n = 10$, $I_m = 1$ A, $Z_0 = 50\ \Omega$, and $\theta = -(\pi/n)$: (a) the magnitude of $I_{r,k}$; (b) the magnitude of V_k; (c) the magnitude, and (d) the power factor of $P_{S,k}$ and $P_{r,k}$.

Let us take an example for $n = 10$, $I_m = 1$, $Z_0 = 50\ \Omega$, and $\theta = -(\pi/n)$. Figure 3(a) and (b) shows that the magnitude of V_k and $I_{r,k}$ gradually increases as the integer k approaches the integer n. The voltage stress across current sources and the current stress carried by a transmission line are strongly indicated from the results of Fig. 3(a)–(b) to be larger, when the sources and TLs are closer to the accumulating target load R_{L2}.

Let $P_{r,k} = \frac{1}{2}V_k\bar{I}_{r,k}$, $P_{l,k} = \frac{1}{2}V_k\bar{I}_{l,k}$ and $P_{S,k} = \frac{1}{2}V_k\bar{I}_{S,k}$ be, respectively, the complex power delivered towards the right transmission line at node k, the complex power delivered towards the left transmission line at node k, and the complex power supplied by the kth current source in Fig. 1, where $\bar{I}$ is defined as the complex conjugate of I. For the given case of $\theta = -(\pi/n)$, by substituting V_k from eq. (8) and $I_{S,k}$ into the definition of $P_{S,k}$, we obtain

$$P_{S,k} = \frac{Z_0 I_m^2}{4}\left(k + \sum_{i=1}^{k} e^{-j\frac{2(n-i)\pi}{n}}\right) \tag{16}$$

$$= \frac{Z_0 I_m^2}{4}\left[k + e^{-j\frac{(n-k+1)\pi}{n}} \frac{\sin\left(\dfrac{n-k}{n}\pi\right)}{\sin\left(\dfrac{\pi}{n}\right)}\right]. \tag{17}$$

The power dissipated by R_{L2}, named P_{L2}, is equal to

$$P_{L2} = \frac{|v_k|^2}{2R_{L2}} = \frac{n^2}{8} Z_0 I_m^2. \tag{18}$$

We can easily verify the fact that P_{L2} is equal to the sum of the real parts of the complex powers supplied by the individual current sources, that is,

$$P_{L2} = \sum_{i=1}^{n} \mathrm{Re}\,(P_{S,k}). \tag{19}$$

Figure 3(c) and (d) illustrates that the power rating and the power factor of $P_{S,k}$ and $P_{r,k}$ for the case of $\theta = -(\pi/n)$ increase as k approaches n. Importantly, the power factors of $P_{S,n}$ and $P_{r,n}$ equal unity. The net power accumulates step by step towards the target load R_{L2}, as indicated from the results of $P_{r,k}$. Another condition for accumulating power toward the other target load R_{L1} is $\theta = \pi/n$, which is verified by the results shown in Fig. 4.

The PV renewable energy can be accumulated and propagated towards either of the terminals via the CT-TLCS in Fig. 1, where the length l of all subTLs is equal to $\lambda/2n$ and the current source $I_{S,k} = I_m \times e^{jk\theta}$ must satisfy the phase conditions $\theta = -(\pi/n)$ or $\theta = \pi/n$.

3. TRANSMISSION-LINE TYPE VOLTAGE SOURCE

Consider the transmission line circuit shown in Fig. 5. To determine the voltage, denoted by $V(x)$, and the current, denoted by $I(x)$, along the TL, the transmission line circuit is partitioned into right and left subtransmission line circuits. Therefore, the voltage and current for the right subtransmission line are

$$V_r(y) = Z_0(i_r^+ e^{-j\beta y} + i_r^- e^{j\beta y}), \tag{20}$$

and

$$I_r(y) = i_r^+ e^{-j\beta y} - i_r^- e^{j\beta y}, \tag{21}$$

and those at the left subtransmission line are

$$V_l(z) = Z_0(i_l^+ e^{-j\beta z} + i_l^- e^{j\beta z}), \tag{22}$$

and

$$I_l(z) = -(i_l^+ e^{-j\beta z} - i_l^- e^{j\beta z}). \tag{23}$$

Now, eqs (20)–(23) must satisfy the following three boundary conditions:

(1) $i_r^- = 0$ holds due to the matching condition of $R_L = Z_0$ at $y = (n-k)\lambda/2n$.

(2) $I_l(0) + I_{S,k} = I_r(0)$ and $V_l(0) = V_r(0)$ hold at

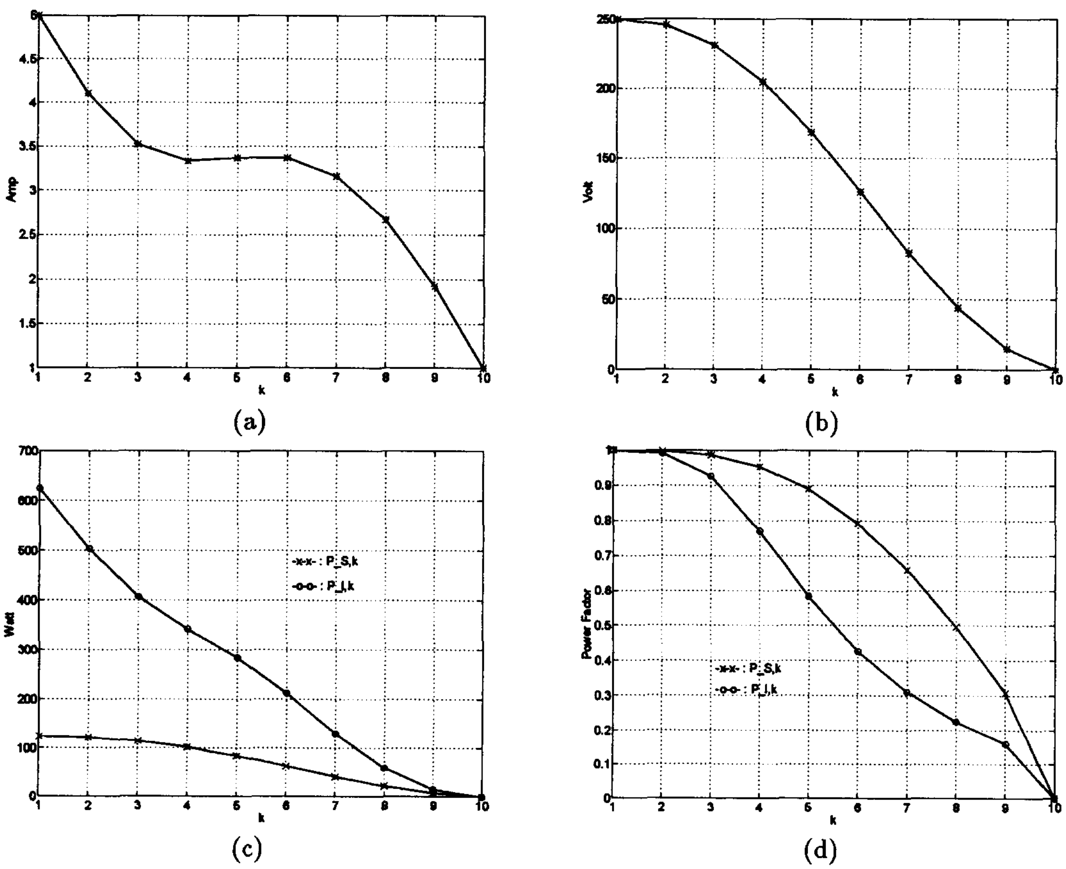

Fig. 4. Simulated results of Fig. 1 under $n = 10$, $I_m = 1$ A, $Z_0 = 50\ \Omega$, and $\theta = \pi/n$: (a) the magnitude of $I_{l,k}$; (b) the magnitude of V_k; (c) the magnitude, and (d) the power factor of $P_{S,k}$ and $P_{l,k}$.

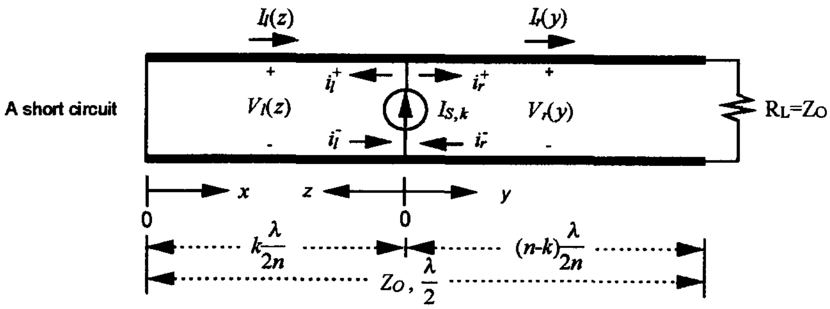

Fig. 5. A transmission line circuit.

$y = 0$ and $z = 0$, therefore we obtain

$$-(i_l^+ - i_l^-) + i_{S,k} = i_r^+ - i_r^-, \tag{24}$$

and

$$Z_0(i_l^+ + i_l^-) = Z_0(i_r^+ + i_r^-). \tag{25}$$

(3) $V_l(z) = 0$ holds at $z = k(\lambda/2n)$. Therefore, we obtain the equation $i_l^+ = -i_l^- \, e^{j2k\phi}$, where $\phi = \beta(\lambda/2n) = \pi/n$.

Now, i_r^+, i_r^-, i_l^+, and i_l^- can be determined further from the above three boundary conditions.

$$i_r^+ = \tfrac{1}{2} I_{S,k}(1 - e^{-j2k\phi}), \tag{26}$$

$$i_r^- = 0, \tag{27}$$

$$i_l^+ = \tfrac{1}{2} I_{S,k}, \tag{28}$$

and

$$i_l^- = -\tfrac{1}{2} e^{-j2k\phi} I_{S,k}. \tag{29}$$

Substituting eqs (26)–(29) into eqs (20)–(23), the voltage and current equations along the subtransmission lines are

$$V_r(y) = \frac{Z_0}{2} I_{S,k}(1 - e^{-j2k\phi})\, e^{-j\beta y}, \tag{30}$$

$$I_r(y) = \tfrac{1}{2} I_{S,k}(1 - e^{-j2k\phi})\, e^{-j\beta y}, \tag{31}$$

$$V_l(z) = \frac{Z_0}{2} I_{S,k}\, e^{-j\beta z} - \frac{Z_0}{2} e^{-j2k\phi} I_{S,k}\, e^{j\beta z}, \tag{32}$$

and

$$I_l(z) = -\tfrac{1}{2} I_{S,k}\, e^{-j\beta z} - \tfrac{1}{2} e^{-j2k\phi} I_{S,k}\, e^{j\beta z}). \tag{33}$$

The voltage $V(x)$ and current $I(x)$ along the TL will be obtained according to whether the position, x, is on the right side or the left side of current source $I_{S,k}$. Therefore, the voltage $V(x)$ and the current $I(x)$ at $x = p(\lambda/2n)$ will be determined as follows:

(1) If $0 \leqslant p < k$, then $z = k\dfrac{\lambda}{2n} - p\dfrac{\lambda}{2n}$.

$$\begin{aligned} V_p &\equiv V(x)|_{x=p\frac{\lambda}{2n}} \\ &= V_l(z)|_{z=k\frac{\lambda}{2n}-p\frac{\lambda}{2n}} \\ &= \frac{Z_0}{2} I_{S,k}\, e^{-j\beta\left(k\frac{\lambda}{2n}-p\frac{\lambda}{2n}\right)} - \frac{Z_0}{2} e^{-j2k\phi} I_{S,k}\, e^{j\beta\left(k\frac{\lambda}{2n}-p\frac{\lambda}{2n}\right)} \\ &= \frac{Z_0}{2} I_{S,k}\, e^{-j(k\phi-p\phi)} - \frac{Z_0}{2} e^{-j2k\phi} I_{S,k}\, e^{j(k\phi-p\phi)} \\ &= jZ_0 \sin(p\phi)\, e^{-jk\phi} I_{S,k}, \end{aligned} \tag{34}$$

and

$$\begin{aligned} I_{r,p} &\equiv I(x)|_{x=p\frac{\lambda}{2n}} \\ &= I_l(z)|_{z=k\frac{\lambda}{2n}-p\frac{\lambda}{2n}} \\ &= -\tfrac{1}{2} I_{S,k}\, e^{-j\beta\left(k\frac{\lambda}{2n}-p\frac{\lambda}{2n}\right)} - \tfrac{1}{2} e^{-j2k\phi} I_{S,k}\, e^{j\beta\left(k\frac{\lambda}{2n}-p\frac{\lambda}{2n}\right)} \\ &= -\tfrac{1}{2} I_{S,k}\, e^{-j(k\phi-p\phi)} - \tfrac{1}{2} e^{-j2k\phi} I_{S,k}\, e^{j(k\phi-p\phi)} \\ &= -\cos(p\phi)\, e^{-jk\phi} I_{S,k}. \end{aligned} \tag{35}$$

(2) If $k \leqslant p \leqslant n$, then $y = p\dfrac{\lambda}{2n} - k\dfrac{\lambda}{2n}$.

$$\begin{aligned} V_p &\equiv V(x)|_{x=p\frac{\lambda}{2n}} \\ &= V_r(z)|_{z=p\frac{\lambda}{2n}-k\frac{\lambda}{2n}} \\ &= \frac{Z_0}{2} I_{S,k}(1 - e^{-j2k\phi})\, e^{-j\beta\left(p\frac{\lambda}{2n}-k\frac{\lambda}{2n}\right)} \\ &= \frac{Z_0}{2} I_{S,k}(1 - e^{-j2k\phi})\, e^{-j(p\phi-k\phi)} \\ &= jZ_0 \sin(k\phi)\, e^{-jp\phi} I_{S,k}, \end{aligned} \tag{36}$$

and

$$I_{r,p} \equiv I(x)\,|_{x=p\frac{\lambda}{2n}}$$

$$= I_{\mathrm{r}}(z)\,|_{z=p\frac{\lambda}{2n}-k\frac{\lambda}{2n}}$$

$$= \mathrm{j}\sin(k\phi)\,\mathrm{e}^{-\mathrm{j}p\phi}I_{\mathrm{S},k}. \qquad (37)$$

Figure 6(a) shows the schematic of a transmission-line type voltage source (TLT-VS), where all current sources are equally spaced from one another. The TLT-VS in Fig. 6(a) can be regarded as a linear system. Based on eqs (34)–(37), the current $I_{\mathrm{r},p}$ and the voltage V_p at port p are really the sum of the responses to individual current sources $I_{\mathrm{S},k}$. $I_{\mathrm{r},p}$ and V_p can be expressed as the form of matrices:

Since $\phi = \pi/n$, the value of j sin $n\phi\mathrm{e}^{-\mathrm{j}n\phi}$ in the (n, n) element of the matrices in eqs (38)(39) is equal to zero. It is important to note that the current $I_{\mathrm{r},n}$ and the voltage V_n at port n are independant of the nth current source $I_{\mathrm{S},n}$ but depend on current sources $I_{\mathrm{S},k}$ for $k = 1, 2, \ldots, n-1$. Hence, the quantity of complex power received by R_{L}, $\frac{1}{2}V_n\bar{I}_{n,r}$, has nothing to do with $I_{\mathrm{S},n}$, therefore, $I_{\mathrm{S},n}$ can be neglected.

Since the input impedance looking towards the TL of length $l = \lambda/2$ with a short circuit is equal to zero, the net equivalent circuit of Fig. 6(a) is obtained by replacing the TL and $I_{\mathrm{S},k}$ for $k = 1, \ldots, n-1$ with one voltage source V_n according to Thevenin's theorem,

$$\begin{bmatrix} I_{\mathrm{r},1} \\ I_{\mathrm{r},2} \\ I_{\mathrm{r},3} \\ \vdots \\ I_{\mathrm{r,n}} \end{bmatrix} = \begin{bmatrix} \mathrm{j}\sin\phi\mathrm{e}^{-\mathrm{j}\phi} & -\cos\phi\mathrm{e}^{-\mathrm{j}2\phi} & -\cos\phi\mathrm{e}^{-\mathrm{j}3\phi} & \ldots & -\cos\phi\mathrm{e}^{-\mathrm{j}n\phi} \\ \mathrm{j}\sin\phi\mathrm{e}^{-\mathrm{j}2\phi} & \mathrm{j}\sin2\phi\mathrm{e}^{-\mathrm{j}2\phi} & -\cos2\phi\mathrm{e}^{-\mathrm{j}3\phi} & \ldots & -\cos2\phi\mathrm{e}^{-\mathrm{j}n\phi} \\ \mathrm{j}\sin\phi\mathrm{e}^{-\mathrm{j}3\phi} & \mathrm{j}\sin2\phi\mathrm{e}^{-\mathrm{j}3\phi} & \mathrm{j}\sin3\phi\mathrm{e}^{-\mathrm{j}3\phi} & \ldots & -\cos3\phi\mathrm{e}^{-\mathrm{j}n\phi} \\ \vdots & \vdots & \vdots & \ddots & \vdots \\ \mathrm{j}\sin\phi\mathrm{e}^{-\mathrm{j}n\phi} & \mathrm{j}\sin2\phi\mathrm{e}^{-\mathrm{j}n\phi} & \mathrm{j}\sin3\phi\mathrm{e}^{-\mathrm{j}n\phi} & \ldots & \mathrm{j}\sin n\phi\mathrm{e}^{-\mathrm{j}n\phi} \end{bmatrix} \begin{bmatrix} I_{\mathrm{S},1} \\ I_{\mathrm{S},2} \\ I_{\mathrm{S},3} \\ \vdots \\ I_{\mathrm{S},n} \end{bmatrix}, \qquad (38)$$

and

$$\begin{bmatrix} V_1 \\ V_2 \\ V_3 \\ \vdots \\ V_n \end{bmatrix} = Z_0 \begin{bmatrix} \mathrm{j}\sin\phi\mathrm{e}^{-\mathrm{j}\phi} & \mathrm{j}\sin\phi\mathrm{e}^{-\mathrm{j}2\phi} & \mathrm{j}\sin\phi\mathrm{e}^{-\mathrm{j}3\phi} & \ldots & \mathrm{j}\sin\phi\mathrm{e}^{-\mathrm{j}n\phi} \\ \mathrm{j}\sin\phi\mathrm{e}^{-\mathrm{j}2\phi} & \mathrm{j}\sin2\phi\mathrm{e}^{-\mathrm{j}2\phi} & \mathrm{j}\sin2\phi\mathrm{e}^{-\mathrm{j}3\phi} & \ldots & \mathrm{j}\sin2\phi\mathrm{e}^{-\mathrm{j}n\phi} \\ \mathrm{j}\sin\phi\mathrm{e}^{-\mathrm{j}3\phi} & \mathrm{j}\sin2\phi\mathrm{e}^{-\mathrm{j}3\phi} & \mathrm{j}\sin3\phi\mathrm{e}^{-\mathrm{j}3\phi} & \ldots & \mathrm{j}\sin3\phi\mathrm{e}^{-\mathrm{j}n\phi} \\ \vdots & \vdots & \vdots & \ddots & \vdots \\ \mathrm{j}\sin\phi\mathrm{e}^{-\mathrm{j}n\phi} & \mathrm{j}\sin2\phi\mathrm{e}^{-\mathrm{j}n\phi} & \mathrm{j}\sin3\phi\mathrm{e}^{-\mathrm{j}n\phi} & \ldots & \mathrm{j}\sin n\phi\mathrm{e}^{-\mathrm{j}n\phi} \end{bmatrix} \begin{bmatrix} I_{\mathrm{S},1} \\ I_{\mathrm{S},2} \\ I_{\mathrm{S},3} \\ \vdots \\ I_{\mathrm{S},n} \end{bmatrix}. \qquad (39)$$

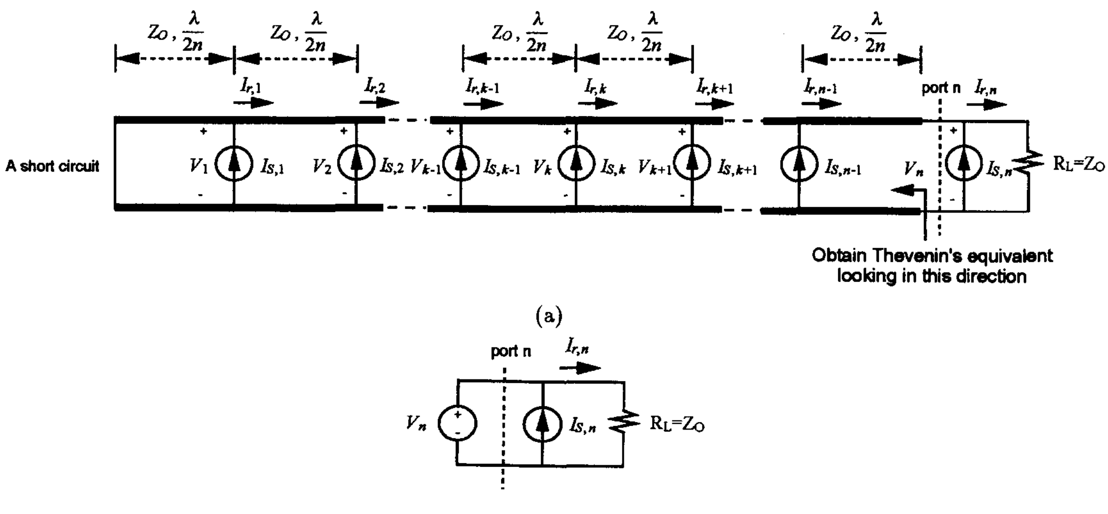

Fig. 6. (a) Transmission-line type voltage source (TLT-VS); (b) Thevenin's equivalent with respect to port n.

as shown in Fig. 6(b). It is emphasized that the TL and $n-1$ current sources $I_{S,k}$ for $k = 1, \ldots, n-1$ in the TLT-VS of Fig. 6(a) act as a voltage source V_n with respect to port n.

Substituting $I_{S,1} = I_{S,2} = \ldots = I_{S,n-1} = I_S$ into eqs (38) and (39), the current $I_{r,n}$ flowing through R_L and the voltage V_n across R_L are

$$I_{r,n} = \sum_{m=1}^{n-1} \mathrm{j} \sin(m\phi)\, \mathrm{e}^{-\mathrm{j}\pi} I_S, \tag{40}$$

and

$$V_n = Z_0 \sum_{m=1}^{n-1} \mathrm{j} \sin(m\phi)\, \mathrm{e}^{-\mathrm{j}\pi} I_S, \tag{41}$$

where $\phi = \pi/n$. Therefore, the desired equivalent voltage phasor V_n can be created by properly selecting current phasor I_S.

4. NETWORK DUALS

The duality principle operates on a circuit or network of two-terminal elements to produce another network with the same number of elements. The original and transformed circuits are said to be duals of each other, and their properties are closely related in many ways. The duality transformation is a two-step process: the first step is a process of interchanging the voltage and current waveforms of each circuit element; the second step is a topological transformation that rearranges the interconnections between elements to obey Kirchhoff's voltage and current laws.

In this section, the voltage-type transmission line collection system (VT-TLCS) and the transmission-line type current source (TLT-CS), which use only distributed voltage sources, can be easily developed from the CT-TLCS of Fig. 1 and the TLT-VS of Fig. 6(a) which contain only current sources.

4.1. *Transmission-line dual*

A segment of transmission line can be regarded as a two-port network and the two-port equations are

$$v_2 = v_1 \cosh(\gamma l) - Z_0 i_1 \sinh(\gamma l), \tag{42}$$

and

$$i_2 = \frac{1}{Z_0}(-v_1 \sinh(\gamma l) + Z_0 i_1 \cosh(\gamma l)). \tag{43}$$

According to the dual transformation, one interchanges the voltage and current waveforms, that is, let v be i^* and i be v^*, and simultaneously the value of G_0^* equals that of Z_0. Then

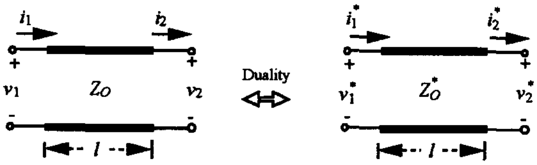

Fig. 7. Dual of transmission line.

$$i_2^* = i_1^* \cosh(\gamma l) - G_0^* v_1^* \sinh(\gamma l), \tag{44}$$

and

$$v_2^* = \frac{1}{G_0^*}(-i_1^* \sinh(\gamma l) + G_0^* v_1^* \cosh(\gamma l)). \tag{45}$$

By letting $Z_0^* = (G_0^*)^{-1}$ and rearranging eqs (61) and (62), one obtains

$$v_2^* = v_1^* \cosh(\gamma l) - Z_0^* i_1^* \sinh(\gamma l), \tag{46}$$

and

$$i_2^* = \frac{1}{Z_0^*}(-v_1^* \sinh(\gamma l) + Z_0^* i_1^* \cosh(\gamma l). \tag{47}$$

Equations (46) and (47) are obviously the same as eqs (42) and (43). Therefore, the dual of a transmission line with characteristic impedance Z_0 is also a transmission line with characteristic impedance Z_0^* numerically equal to Z_0^{-1}, as shown in Fig. 7.

4.2. *Topological duals*

The second part of the duality transformation—formation of the structural dual—transforms the topological structure of the network such that meshes and nodes are interchanged. This step ensures that the dual network satisfies Kirchhoff's voltage and current laws. The algorithm for finding the topological dual is well known and can be found in texts on basic network theory [5]. Figure 8 illustrates that a collection system using current sources is transformed into one using voltage sources by using the transmission line dual and rearranging interconnection between dual elements. Based on the duality principle previously discussed, the voltage-type transmission line collection system (VT-TLCS) can be easily developed from the CT-TLCS of Fig. 1, as shown in

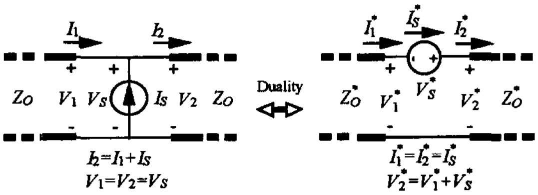

Fig. 8. Example of applying the duality principle to collection systems.

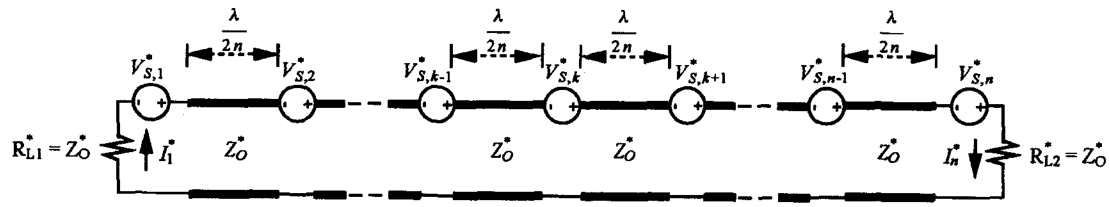

Fig. 9. Voltage-type transmission line collection system (VT-TLCS).

Fig. 9, where the phasor representative of the voltage source is $V^*_{S,k} = V_m e^{jk\theta}$ and both terminals satisfy $R^*_{L1} = R^*_{L2} = Z^*_0$. It is noted that the characteristic impedance Z^*_0 numerically equals Z_0^{-1}. The voltage and current waveforms of both transmission line collection systems are interchanged with each other. By controlling the phase degree of θ, the net power flow can be toward either of the terminals R_{L1} or R_{L2}. Therefore, for the case of $\theta = -(\pi/n)$, the current I^*_1 through R^*_{L1} equals zero and the current I^*_n through R^*_{L2} can be obtained by interchanging the voltage and current waveforms of eq. (12):

$$I^*_n = \frac{n}{2Z^*_0} V_m e^{jn\theta}. \tag{48}$$

Similarly, the transmission-line type current source (TLT-CS) can be derived from the TLT-VS in Fig. 6 by utilization of the duality algorithm, as illustrated in Fig. 10, where the phasor representative of every source is V^*_S and the terminal R^*_L equals Z^*_0. Since the input impedance looking towards the TL of length $l = \lambda/2$ with an open circuit is equal to infinity, Norton's equivalent of the TLT-CS, with respect to port n, is shown in Fig. 10(b). The TLT-CS of Fig. 10 acts as a current source I^*_n with respect to the nth port. The relationship between I^*_n and V^*_S for the TLT-CS can be obtained by interchanging the voltage and current waveforms of eq. (41):

$$I^*_n = \frac{1}{Z^*_0} \sum_{m=1}^{n-1} j \sin(m\phi) e^{-j\pi} V^*_S, \tag{49}$$

where $\phi = (\pi/n)$. The equivalent current flow I^*_n is

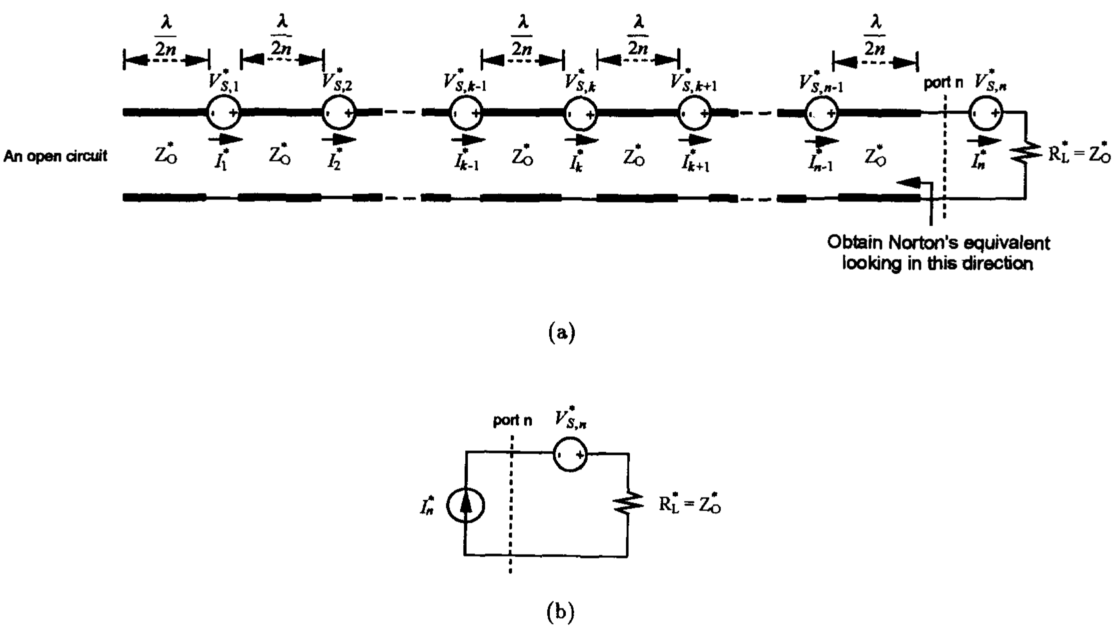

Fig. 10. (a) Transmission-line type current source (TLT-CS); (b) Norton's equivalent with respect to port n.

determined by properly choosing the voltage phasor V_S^*.

5. TWO-DIMENSIONAL COLLECTION SYSTEMS

Natural energy is indeed distributed over a wide area, and two-dimensional collection systems facilitate the collection of the distributed energy. Two-dimensional transmission-line collection systems (2D-TLCSs) can be simply derived from the CT-TLCS or VT-TLCS by replacing distributed a.c. electric sources with TLT-VSs or TLT-CSs.

Figure 11 illustrates a schematic of a two-dimensional voltage-type transmission line collection system (2D-VT-TLCS), where the main collection system is one CT-TLCS with the distributed a.c. current sources $I_{S,k} = I_M e^{jk\theta}$ and every distributed a.c. current source is created by a TLT-CS. It is noted that the characteristic impedance of the main TL, denoted by Z_{0m}, is equal to 2 times that of the subTL, denoted by Z_{0s}, that is, $Z_{0m} = 2Z_{0s}$. $V_{S,k,h}$ denotes the hth voltage source in the kth TLT-CS. As previously discussed, all of the voltage sources in the kth TLT-CS are the same and can be determined from eq. (49) for the given $I_{S,k}$:

$$V_{S,k,h} = \frac{Z_{0s} I_{S,k}}{\sum_{i=1}^{n-1} j \sin(i\phi)\, e^{-j\pi}} = jZ_{0s} \frac{I_M e^{jk\theta}}{\sum_{i=1}^{n-1} \sin\left(\frac{i\pi}{n}\right)}. \tag{50}$$

For a given case of $\theta = -(\pi/q)$, the main collection network accumulates all of the average power supplied by sources toward R_{L2} but R_{L1} will receive no power, as analyzed in Section 2. The voltage across R_{L1} is zero and the voltage phasor V_q across R_{L2} is described by eq. (12):

$$V_q = \frac{q}{2} Z_{0m} I_M e^{-j\pi}. \tag{51}$$

$P_{S,k,h} = \frac{1}{2} V_{S,k,h} \bar{I}_{k,h}$ is defined as the complex power supplied by voltage source $V_{S,k,h}$, where $I_{k,h}$ is the current

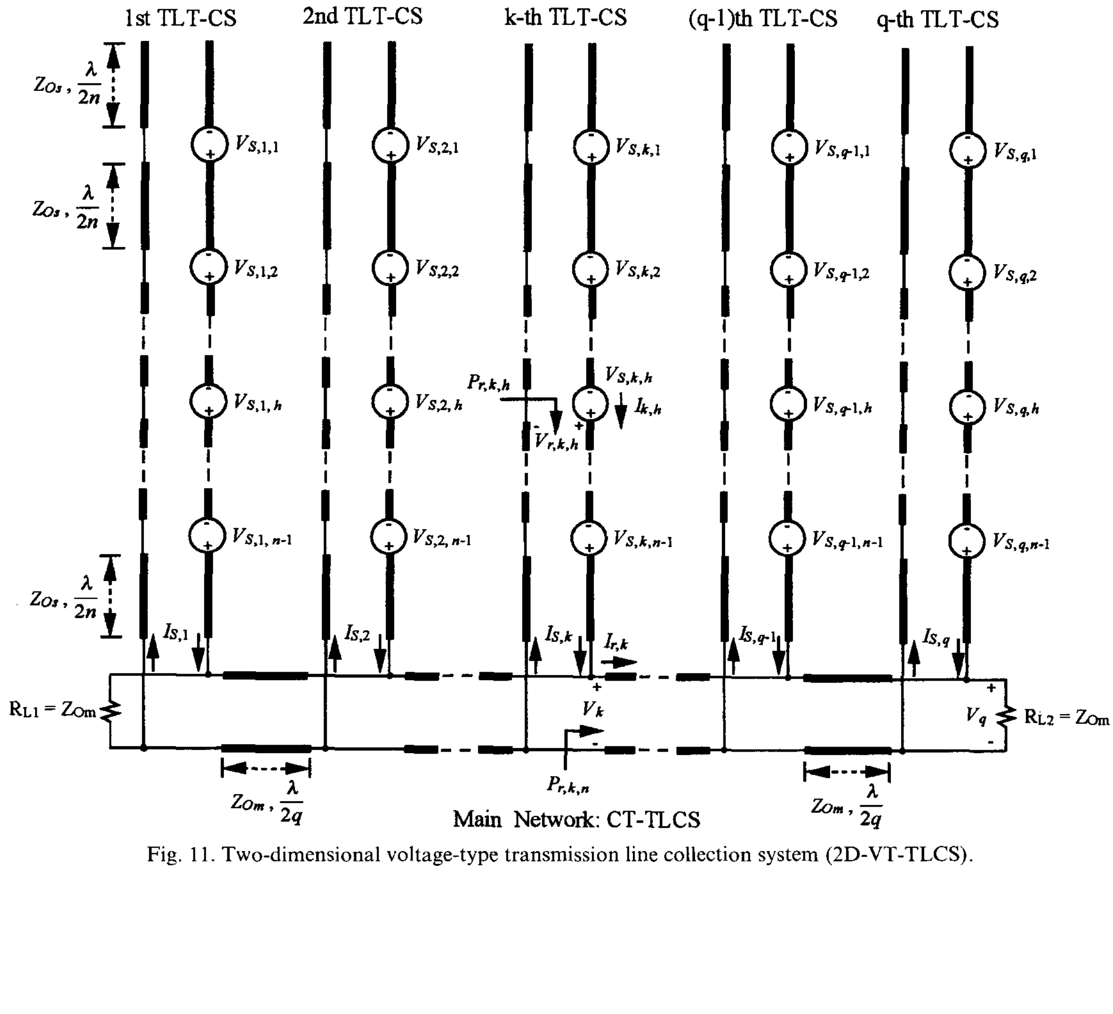

Fig. 11. Two-dimensional voltage-type transmission line collection system (2D-VT-TLCS).

through voltage source $V_{S,k,h}$. $P_{r,k,h} = \frac{1}{2}V_{r,k,h}\bar{I}_{k,h}$ is also defined as the complex power looking toward the main network at the kth TLT-CS. Moreover, $P_{r,k,n} = \frac{1}{2}V_k\bar{I}_{r,k}$ is defined as the complex power looking towards R_{L2} at the main network.

The simulated results of Fig. 11 with $Z_{0m} = 50\ \Omega$, $Z_{0s} = 25\ \Omega$, $n = 10$, $q = 10$, and $I_{S,k} = 10\,e^{-j(k\pi/q)}$A are illustrated in Fig. 13. The voltage stress across the sub-TLs in the TLT-CSs is minimal at the middle but is maximal at both sides of the TLT-CS, as shown in Fig. 13(a). In contrast, the current stress through voltage source in the TLT-CS as shown in Fig. 13(b) appears to be at a maximum at the middle but has a minimum at both sides of the TLT-CS. As observed from Fig. 13(c)–(d), the power rating and power factor of voltage sources in the TLT-CS increase as the location of the TLT-CS is closer to the target load R_{L2}. It is emphasized that the two-dimensional transmission-line network can propagate energy toward the target load R_{L2} and can store energy in the form of electric field or magnetic field, as illustrated by Fig. 13(e)–(f). The real part of $P_{r,k,h}$ increases as $k \to q$ and/or $h \to n$, that is, the net power can be accumulated and transmitted towards the target load R_{L2} via the proposed 2D-VT-TLCS, as described by the results shown in Fig. 13(e).

Similarly, Fig. 12 shows a schematic of a two-dimensional current-type transmission line collection system (2D-CT-TLCS) that adopts one VT-TLCS as the main collection system and constructs every distributed a.c. voltage source $V_{S,k} = V_M e^{jk\theta}$ in the main VT-TLCS by using TLT-VSs, where the characteristic impedance of the main TL is equal to half that of the subTL, that is, $Z_{0m} = \frac{1}{2}Z_{0s}$. The symbol $I_{S,k,h}$ is defined as the hth current source in the kth TLT-VS. All of the current sources in the kth TLT-VS are identical and can be obtained from eq. (41):

$$I_{S,k,h} = \frac{V_{S,k}}{Z_{0s}\sum_{i=1}^{n-1} \mathrm{j}\sin(i\phi)\,e^{-\mathrm{j}\pi}} = \mathrm{j}\frac{V_M\,e^{\mathrm{j}k\theta}}{Z_{0s}\sum_{i=1}^{n-1}\sin\left(\frac{i\pi}{n}\right)}. \tag{52}$$

It is emphasized that the 2D-VT-TLCS and 2D-CT-

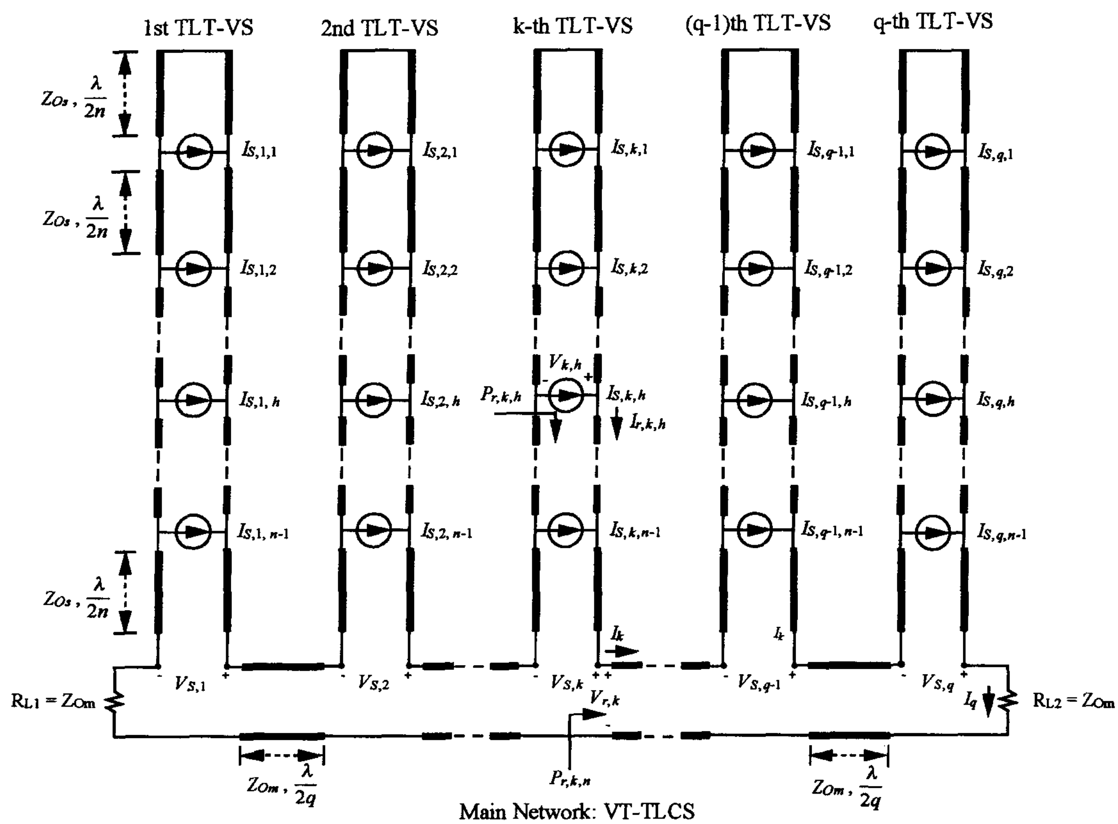

Fig. 12. Two-dimensional current-type transmission line collection system (2D-CT-TLCS).

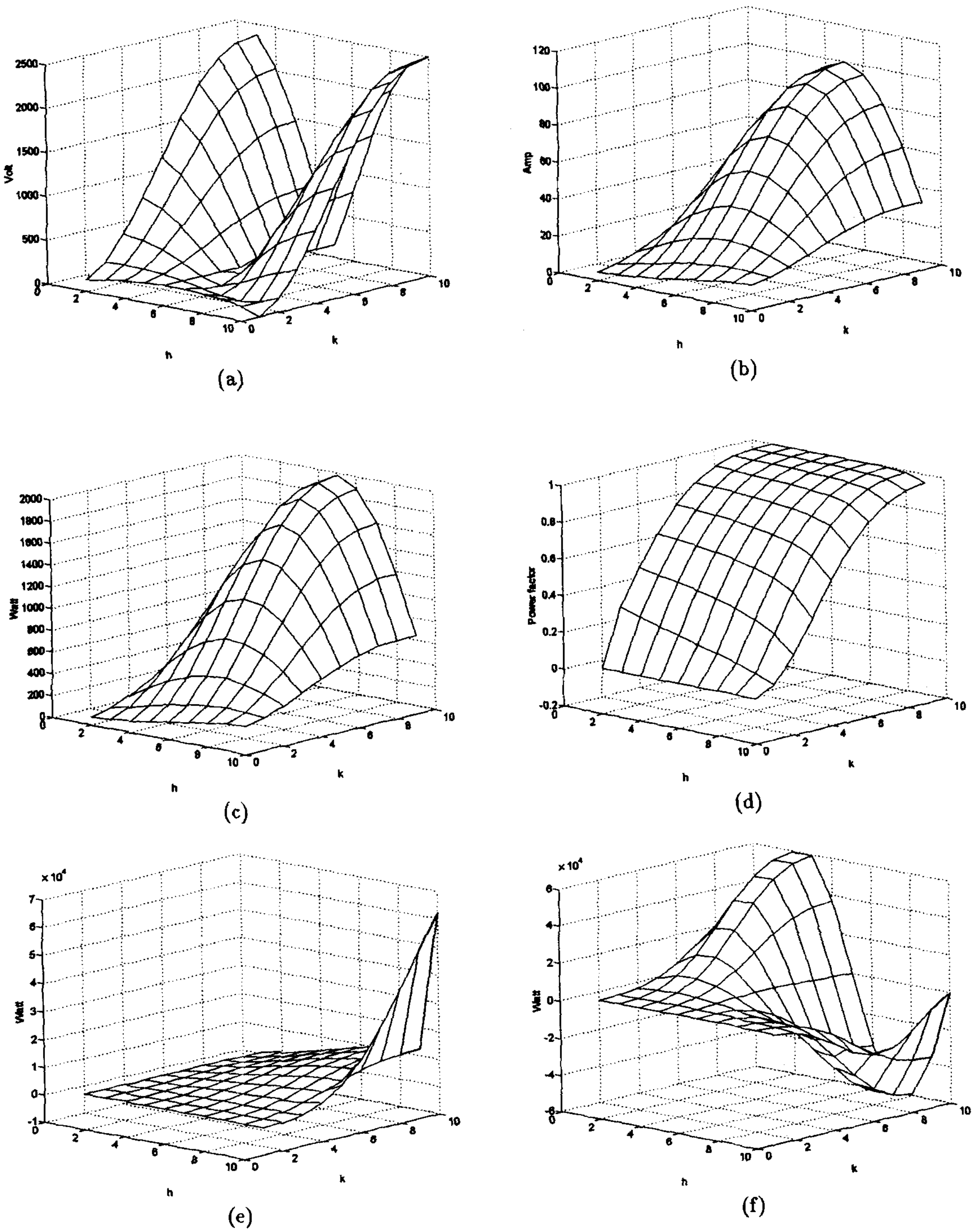

Fig. 13. Simulated results of Fig. 11 under $Z_{0m} = 50\ \Omega$, $Z_{0s} = 25\ \Omega$, $n = 10$, $q = 10$, and $I_{S,k} = 10\,e^{-j(k\pi/q)}$A. (a) The magnitude of $V_{r,k,h}$; (b) the magnitude of $I_{k,h}$; (c) the magnitude, and (d) the power factor of $P_{S,k,h}$; (e) the real part, and (f) the imaginary part of $P_{r,k,h}$.

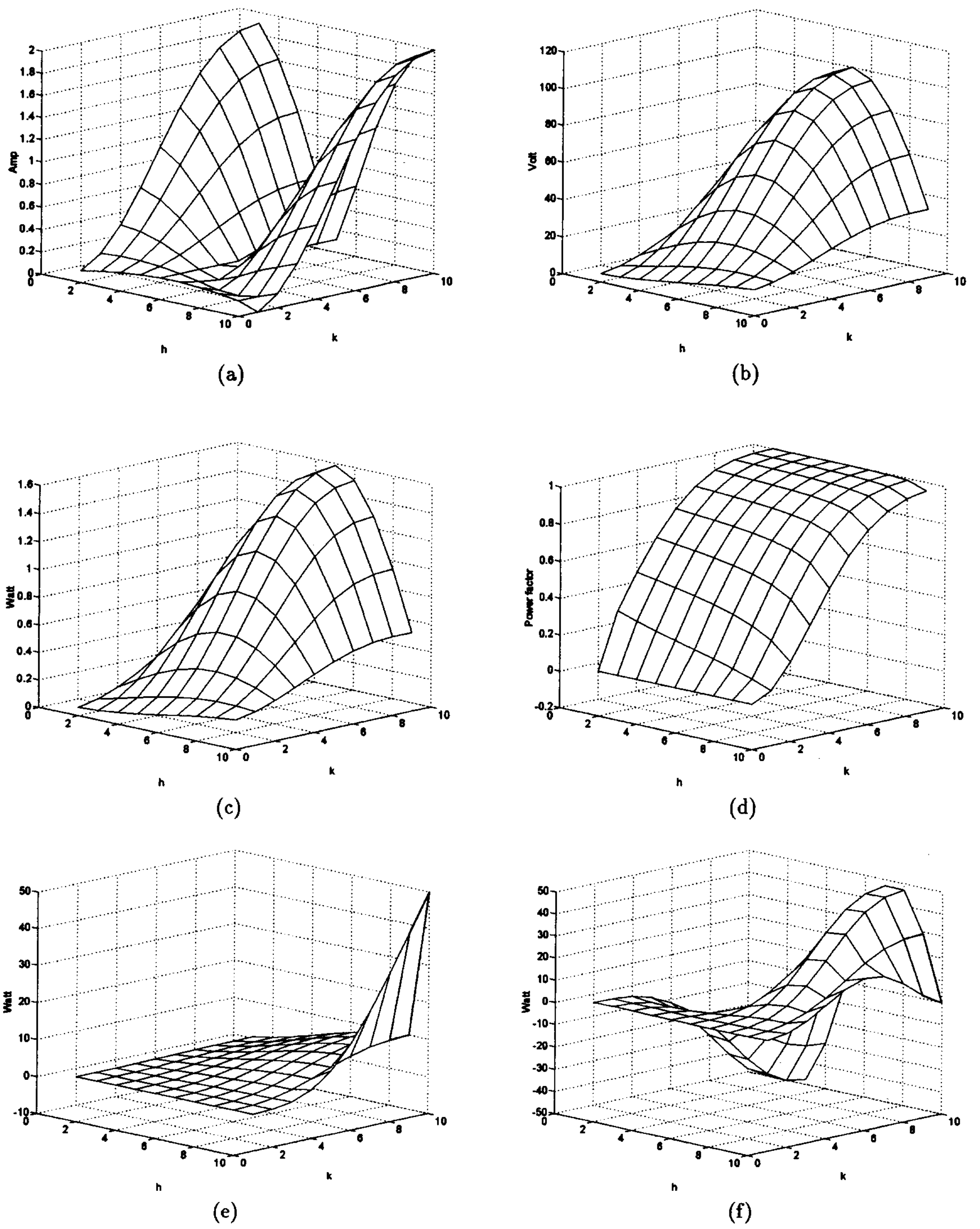

Fig. 14. Simulated results of Fig. 12 under $Z_{0m} = 25\ \Omega$, $Z_{0s} = 50\ \Omega$, $n = 10$, $q = 10$, and $V_{S,k} = 10\,e^{-j(k\pi/q)}$ V. (a) The magnitude of $I_{r,k,h}$; (b) the magnitude of $V_{k,h}$; (c) the magnitude, and (d) the power factor of $P_{S,k,h}$; (e) the real part, and (f) the imaginary part of $P_{r,k,h}$.

TLCS are duals of each other, that is, the current and voltage waveforms between both collection systems in Fig. 11 and Fig. 12 are interchanged with each other. Consequently, for a given case of $\theta = -(\pi/q)$, the main collection network accumulates all of the average power supplied by the sources toward R_{L2} but R_{L1} will receive no power. The current through R_{L1} is zero and the current phasor I_q through R_{L2} is obtained from eq. (48):

$$I_q = \frac{q}{2Z_{0m}} V_M \, e^{-j\pi}. \tag{53}$$

$P_{S,k,h} = \frac{1}{2} V_{k,h} \bar{I}_{S,k,h}$ is defined as the complex power supplied by voltage source $V_{k,h}$, where $V_{k,h}$ is the voltage across current source $I_{S,k,h}$. $P_{r,k,h} = \frac{1}{2} V_{k,h} \bar{I}_{r,k,h}$ is also defined as the complex power looking towards the main network at the kth TLT-VS. Additionally, $P_{r,k,n} = \frac{1}{2} V_{r,k} \bar{I}_k$ is defined as the complex power looking towards R_{L2} at the main network. Figure 14 shows the simulated results of Fig. 12 under $Z_{0m} = 25\ \Omega$, $Z_{0s} = 50\ \Omega$, $n = 10$, $q = 10$, and $V_{S,k} = 10\, e^{-j(k\pi/q)}$ V. The current and voltage characteristics of 2D-CT-TLCSs are, respectively, the same as the voltage and current characteristics of 2D-VT-TLCSs as they are duals of each other, confirmed by comparing Fig. 14(a)–(d) with Fig. 13(a)–(d). The significance of this is that the function of accumulating energy toward the target load R_{L2} is verified by the simulated result of Fig. 14(e).

6. CONCLUSIONS

The purpose of this paper is to propose two-dimensional transmission-line collection systems for accumulating renewable PV energy distributed over a very large region and transmitting it towards the target load. Both two-dimensional current-type and voltage-type transmission-line collection systems for collecting the distributed PV power have been presented in this paper. Based on transmission line theory and controlling the phase of a.c. sources, the net power of the proposed transmission-line type networks can flow towards the target load. Moreover, the proposed novel 2D-VT-TLCS and 2D-CS-TLCS cost less because only those sources close to the target load are required to have a large power rating. It is expected that the energy collected from the distributed PV sources will therefore be relatively cheap.

REFERENCES

1. E. Edelson, Photovoltaics: solar cell update. *Popular Science*, pp. 95–99 (June 1992).
2. F. Lasnier and T. G. Ang, *Photovoltaic Engineering Handbook*, Adam Hilger, Bristol, pp. 83–97 (1990).
3. S. M. M. Woff and J. H. R. Enslin, Economical, PV maximum power point tracking regulator with simplistic controller. *Proc. 24th Annual IEEE Power Electronics Specialists Conference*, PESC'93, pp. 581–587 (1993).
4. D. K. Cheng, *Field and Wave Electromagnetics*, pp. 427–508. Addison-Wesley, Reading, MA (1989).
5. C. Desoer and E. Kuh, *Basic Circuit Theory*. McGraw Hill, New York (1969).